Tellus (2003), 55B, 35–53
Printed in UK. All rights reserved

TELLUS
ISSN 0280–6509

Cloud condensation nuclei spectra derived from size distributions and hygroscopic properties of the aerosol in coastal south-west Portugal during ACE-2

By ULRIKE DUSEK[1]*, DAVID S. COVERT[1], ALFRED WIEDENSOHLER[2], CHRISTIAN NEUSÜSS[2], DIANA WEISE[2] and WILL CANTRELL[3], [1]*Department of Atmospheric Sciences, Box 351640, University of Washington, Seattle, WA 98105, USA;* [2]*Institut für Troposphärenforschung e.V., Permoserstrasse 15, 04318 Leipzig, Germany;* [3]*Department of Physics, Michigan Technological University, Houghton MI 49931, USA*

(Manuscript received 20 August 2001; in final form 9 October 2002)

ABSTRACT

In this work we propose and test a method to calculate cloud condensation nuclei (CCN) spectra based on aerosol number size distributions and hygroscopic growth factors. Sensitivity studies show that this method can be used in a wide variety of conditions except when the aerosol consist mainly of organic compounds. One crucial step in the calculations, estimating soluble ions in an aerosol particle based on hygroscopic growth factors, is tested in an internal hygroscopic consistency study. The results show that during the second Aerosol Characterization Experiment (ACE-2) the number concentration of inorganic ions analyzed in impactor samples could be reproduced from measured growth factors within the measurement uncertainties at the measurement site in Sagres, Portugal.

CCN spectra were calculated based on data from the ACE-2 field experiment at the Sagres site. The calculations overestimate measured CCN spectra on average by approximately 30%, which is comparable to the uncertainties in measurements and calculations at supersaturations below 0.5%. The calculated CCN spectra were averaged over time periods when Sagres received clean air masses and air masses influenced by aged and recent pollution. Pollution outbreaks enhance the CCN concentrations at supersaturations near 0.2% by a factor of 3 (aged pollution) to 5 (recent pollution) compared to the clean marine background concentrations. In polluted air masses, the shape of the CCN spectra changes. The clean spectra can be approximated by a power function, whereas the polluted spectra are better approximated by an error function.

1. Introduction

Stratus clouds, which cover large parts of the oceans are important for the radiative balance of the global atmosphere. At visible wavelengths stratus clouds have a much higher albedo than the underlying ocean surface and reflect more solar radiation back to space, while the long-wave radiation emitted by those low cloud systems is comparable to that of the ocean surface. Stratus clouds have thus a net cooling effect on the climate. It has been proposed (e.g. Twomey et al., 1987; Twomey, 1991) that the albedo of stratus clouds is to some extent controlled by the number concentration of the aerosol particles that serve as nucleation sites for the cloud droplets. An increase in aerosol number concentrations may result in clouds with more, but smaller droplets and a higher albedo, which enhances their cooling effect on the climate system. The increase of cloud albedo caused by an increase in aerosol concentrations is commonly referred to as the indirect effect of aerosols on climate. This effect has been confirmed by experimental evidence. This includes measurements of aerosol and cloud properties in ship tracks (e.g. Ferek et al., 1998), changes in the relationship of long- and short-wave cloud

*Corresponding author.
e-mail: uli@atmos.washington.edu

reflectance due to pollution outbreaks from the European continent during ACE-2 (Brenguier et al., 2000), and seasonal differences in stratus clouds off the coast of Australia, that can be explained by fluctuations in the natural background aerosol (Boers et al., 1998).

The quantification of the indirect effect has as yet large uncertainties, but its existence is quite well established locally. Thus it can be expected that globally an increase in aerosol number concentrations by anthropogenic emissions could result in a negative radiative forcing of the climate system (e.g. Charlson et al., 1992) by increasing the particle concentrations in areas where the background concentrations are low. These are the areas where the cloud albedo is expected to be most sensitive to anthropogenic influence. However, it is difficult to quantify this anthropogenic indirect forcing and to relate a change in global cloud albedo to the anthropogenic increase in aerosol mass or number concentrations. One of the complications is that cloud droplets nucleate only on a subset of all aerosol particles. The identification of this subset of the aerosol population can thus be considered a first step in linking the indirect radiative forcing to total aerosol number or mass concentration.

The concept of cloud condensation nuclei (CCN) has been useful in this context. CCN are usually defined as the aerosol particles that 'activate' (i.e. grow by water uptake that is kinetically rather than thermodynamically limited) at a certain supersaturation (S). This concept inherently involves the assumption that prior to activation the droplets are in equilibrium with the surrounding water vapor. If this assumption is justified the number concentration of activated particles is only dependent on the maximum supersaturation and not on the history of S. Whether this equilibrium assumption is valid in ambient clouds is still a subject under study (e.g. Chuang et al., 1997; Nenes et al., 2001). CCN are usually measured using CCN counters (e.g. Hudson, 1989). In these instruments the aerosol is subjected to a defined S and particles that grow to the sizes of cloud droplets are counted as CCN. CCN can also be calculated using Koehler theory, if the number–size distribution and chemical composition of the aerosol particles are known.

In this investigation we propose and test a method to calculate CCN spectra (i.e. the CCN as a function of S) based on measured particle size distributions and hygroscopic properties. Subsequently, we present calculated CCN spectra for the ACE-2 measurement period from 16 June to 24 July 1997 in Sagres, Portugal (Raes et al., 2000; Verver et al., 2000). In the past and also during the ACE-2 experiment calculated and measured CCN concentrations have often been found to disagree strongly by factors of up to 5 (Chuang et al., 2000; Wood et al., 2000; Snider and Brenguier, 2000). During ACE-2 some of the measured CCN spectra could be explained with very low soluble fractions in the aerosol particles (Raes et al., 2000), but this is in contradiction to hygroscopic growth factor measurements (Swietlicki et al., 2000). To shed more light on this problem we will test the consistency of measured hygroscopic growth factors and chemical composition of the particles. We will also compare the calculated CCN spectra to CCN spectra measured by a new type of instrument called a Cloud Condensation Nucleus Remover (CCNR) described and evaluated by Ji et al. (1998). Moreover, we will include extensive sensitivity studies to investigate a possible influence of organic compounds on the CCN spectra.

The data from the measurement site in Sagres offer the opportunity to study the aerosol characteristics in various air mass types ranging from marine background to continentally polluted conditions. One further objective of this work is to complement the limited number of measured CCN spectra with a data set of calculated CCN spectra that covers the whole ACE-2 measurement period. This allows us to compare CCN spectra in different air mass types and to estimate how much the marine background CCN concentrations are increased by anthropogenic pollution.

2. Calculation of CCN spectra using number size distributions and hygroscopic growth factors

The equilibrium droplet size and cloud nucleating properties of an aerosol particle at cloud humidities are most commonly described by the Koehler theory (e.g. Pruppbacher and Klett, 1997). According to Koehler theory each particle is characterized by a critical water vapor supersaturation (S_c). If the ambient supersaturation (S_a) in a cloud exceeds S_c the particle will become 'activated', i.e. it will grow to the size of a cloud droplet by water uptake that is kinetically rather than thermodynamically limited.

The classical Koehler theory is valid for aerosol particles consisting of water-soluble inorganic salts and an insoluble core. For particles containing significant

soluble material (more than 20%) S_c is to a first approximation only dependent on the number of soluble ions and molecules (N_i) in the particle, and the influence of the insoluble core can be neglected. In this case S_c can be written as

$$S_c = \left(\frac{4A^3}{27BN_i} \right)^{0.5}, \quad (1)$$

where $A = 3.3 \times 10^{-7}/T$, $B = 4.3 \times 10^{-6}$, and T is the ambient temperature [cf. Seinfeld and Pandis (1998, p. 787)]. The classical Koehler theory neglects the influence of soluble and slightly soluble organic substances on the particle water uptake. However, there is empirical evidence that organic aerosols contribute to the CCN concentrations (e.g. Novakov and Penner, 1993; Novakov and Corrigan, 1996). Significant modifications to the Koehler theory to incorporate the effect of slightly soluble and surfactant organic substances and the uptake of soluble gases have been developed recently (Laaksonen et al., 1998; Shulman et al., 1996; Kulmala et al., 1997). Currently it is not possible to consider this influence of organics in the calculation of CCN spectra directly. Only a small fraction of the organic species in the ambient aerosol has been analyzed and classified so far (e.g. Rogge et al., 1993), and the solubility and effects on surface tension of organic species are largely unknown (Saxena and Hildemann, 1996). The CCN spectra presented in this study are therefore calculated using classical Koehler theory. Possible errors which may result from the neglect of organic species in the calculations are estimated in a sensitivity study in section 2.2.

This section shows how the number of soluble species (ions and molecules) in a particle and consequently S_c can be estimated from its hygroscopic growth factor at high relative humidities (r.h.) near 90%. The number of ions and molecules per particle can in principle also be estimated more directly by analyzing inorganic and organic compounds collected on filter or impactor samples of the aerosol. However, those measurement methods have generally poor size resolution, incomplete chemical analysis, and require measurement times of the order of hours. On the other hand, hygroscopic growth factors can be measured directly by a Tandem Differential Mobility Analyzer (TDMA) (Rader and McMurry, 1986), which has a very fine size resolution, and the time to complete one growth factor measurement is approximately 10 min.

2.1. *Estimation of droplet size and* S_c *from hygroscopic growth factors*

A common measure for the hygroscopic growth of an aerosol particle is the diameter growth factor (G), defined as the ratio of the hydrated particle diameter at some specified relative humidity (r.h.) to the dry particle diameter. The growth factors used in this study have been measured by a Tandem Differential Mobility Analyzer (TDMA), which is an instrument widely used in both laboratory and field studies to determine growth factors (e.g. Covert and Heintzenberg, 1993; Swietlicki et al., 2000). A TDMA consists of two Differential Mobility Analyzers (DMA1 and DMA2) that are in series and a humidifying system that conditions the aerosol between DMA1 and DMA2. DMA1 is operated at an r.h. lower than 10% and selects dry aerosol particles within a narrow size range. This size range is determined by the transfer function of DMA1, which is ideally triangular with a diameter range of $\pm 10\%$ or less of the mean diameter (d_0) depending on the DMA1 flow rates (e.g. Martinsson et al., 2001). This quasi-monodisperse aerosol is then subjected to a specified, higher r.h. in the humidifier and finally enters DMA2. Hygroscopic aerosol particles grow by hydration in the humidifier to an equilibrium size that depends on the r.h. and the amount and the chemical nature of the hygroscopic material in the particles. DMA2 scans the resulting size distribution of the hydrated aerosol. This distribution shows an increase in size compared to d_0 and it is usually broadened due to differences in the hygroscopic growth of individual particles. It can have one or more modes if the aerosol consists of particle fractions with distinctly different hygroscopic behavior. The scans of the wet size distribution are inverted using a fitting routine to obtain the mean growth factor (G), standard deviation, and the relative number fraction of each growth mode [TDMAfit; Stolzenburg and McMurry (1988)]. The mean growth factors of each growth mode were used in the following calculations. The growth distributions are mostly symmetric around the mean growth factor for each growth mode. Sensitivity studies show that soluble volume fractions derived from hygroscopic growth factors change less than five percent when the mean growth factors are used in the calculations instead of the whole growth distribution. Thus, this simplification is not expected to change the results of this study significantly.

In this study growth factors measured at 90% r.h. are used to estimate the number of soluble ions and molecules in an atmospheric particle by calculating

the mass of a known model salt that is required to give the same growth factor. This determines the number of soluble ions in the model particle which is 'equivalent' to the number of soluble molecules and ions in the atmospheric aerosol. We term this equivalent ions.

If the model salt is fully dissolved at 90% r.h., the number of equivalent ions can be calculated as the product of the mass of water (m_w) contained in the droplet and the molality of the solution (η):

$$N_i^{eq} = i\eta m_w, \tag{2}$$

where i is the number of ions in which the salt can dissociate. m_w and η can be estimated using the hygroscopic growth factor and empirical formulas that describe the water activity of concentrated electrolytic solutions.

Assuming spherical particle shape, the mass of water contained in an aerosol particle at 90% r.h. can be calculated from the measured hygroscopic growth factor (G) at 90% r.h.:

$$\begin{aligned} m_w &= \rho_w V_w = \rho_w (V_{tot} - V_{dry}) \\ &= \frac{\rho_w \pi}{6}\left[(G d_{dry})^3 - d_{dry}^3\right] = \frac{\pi d_{dry}^3 (G^3 - 1)\rho_w}{6}, \end{aligned} \tag{3}$$

where d_{dry} is the dry particle diameter and ρ_w the density of water. This equation is valid under the assumption that the volumes of water and dissolved species are additive, i.e. that the volume of the particle at 90% r.h. (V_{tot}) is the sum of the dry particle volume (V_{dry}) and the volume of water condensing on the particle (V_w).

The calculation of the molality η is not so straight forward. The aerosol droplets at 90% r.h. are fairly concentrated, so that non-ideal solution effects have to be considered. The vapor pressure over the droplet surface is not only a function of the number concentration of ions in the solution, but also of the specific salt present. This information, however, cannot be obtained through growth factor measurements alone. This is the reason we choose a model salt [e.g. ammonium sulfate, $(NH_4)_2SO_4$] to estimate equivalent ions. For such a model salt it is possible to calculate the molality η of the solution droplet at 90% r.h. with the help of an empirical relationship between η and the water activity (a_w).

In this work we follow an approach by Swietlicki et al. (1999) and use an empirical formula for the molality of a $(NH_4)_2SO_4$ solution determined by Potukuchi and Wexler (1995):

$$\begin{aligned} \eta = {} & 135.9 - 464.03 a_w + 492.36 a_w^2 + 94.33 a_w^3 \\ & - 459.29 a_w^4 + 200.7 a_w^5. \end{aligned} \tag{4}$$

For small solution droplets the water activity (a_w) is related to the ambient r.h. as follows:

$$a_w = \text{r.h.} \times \exp\left(-\frac{4\sigma M_w}{\rho R T G d_{dry}}\right), \tag{5}$$

where σ is the surface tension of the solution, M_w and ρ_w the molecular weight and density of water, R the universal gas constant, T the temperature, and G and d_{dry} the growth factor and dry diameter of the aerosol particle.

Combining eqs. (2)–(5) it is possible to calculate the equivalent number of ions (N_i^{eq}) in a particle, i.e. the number of ions of ammonium sulfate that would produce the observed hygroscopic growth at 90% r.h.. Using N_i^{eq} in eq. (1) the critical supersaturation S_c for any particle can be estimated from the knowledge of its dry diameter and the hygroscopic growth factor at high humidities. If hygroscopic salts other than ammonium sulfate or slightly soluble materials contribute to the hygroscopic growth at 90% r.h. N_i^{eq} is not necessarily equal to the actual number of soluble molecules or ions in the particle. However, estimating the actual number of ions in the particle is not the goal of this study. The equivalent ion number concentration is used as a tool to extrapolate the hygroscopic behavior of the particle as measured at 90% r.h. to higher humidity and supersaturations. This approach uses one main assumption: The ratio between water uptake of the actual soluble material in the particle at 90% r.h. and at S_c is similar to that of ammonium sulfate. If this is not the case errors can be introduced in the calculation of the critical supersaturation. The potential magnitudes of these errors are estimated in the next section.

2.2. *Sensitivity studies*

There are several reasons that the ratio between water uptake at 90% r.h. and water uptake at S_c of an actual particle might differ from that of ammonium sulfate, which is used to calculate equivalent ions, S_c and finally CCN spectra in this study. The hygroscopic material in the particle might be an inorganic salt other than ammonium sulfate. The particle may contain some slightly soluble material that is only partially dissolved at 90% r.h. but dissolves fully at higher supersaturations. The surface tension of the particle could be different at 90% r.h. and at S_c. Soluble gases dissolve in the diluted particle near S_c but not at 90% r.h..

The sensitivity studies presented in this section have two major objectives: The first is to explore a wide variety of aerosol compositions to see in which cases the method of calculating CCN concentrations described in this work can be used. The second is more specifically to investigate if this method is applicable to the conditions in Sagres during ACE-2. A quantitative treatment can only be attempted regarding the effects of inorganic and soluble organic species. The uncertainties associated the uptake of soluble gases are too large to attempt a meaningful quantification and are thus only discussed qualitatively.

2.2.1. Inorganic compounds. If the water activity of the solution at 90% r.h. can be approximated by Raoult's law (ideal solution), S_c is independent of the salt used to calculate N_i^{eq}. Errors in S_c are thus only due to differences in the nonideal solution effects among different inorganic salts at 90% r.h.. For sulfate compounds [such as NH_4HSO_4, $(NH_4)_2SO_4$ or Na_2SO_4] these differences are generally small, and it can be shown that S_c is fairly insensitive to the specific hygroscopic salt used in the calculation of N_i^{eq}. For example if eq. 4 is replaced by a similar empirical expression for ammonium bisulfate (Tang and Munkelwitz, 1994) the resulting number of ions differs less than 10% from N_i^{eq} obtained by using ammonium sulfate. This corresponds to a relative difference in S_c of less than 3% (i.e. an absolute difference of 0.0003 at $S_c = 0.01$) for an assumed particle composition of ammonium sulfate vs. ammonium bisulfate and does not result in any significant difference in the calculated CCN concentrations. For sea salt (or pure NaCl) particles the errors in CCN concentrations can be larger (approximately 25%), if the equivalent ions are calculated using the empirical expression for ammonium sulfate. These possible errors, however, are of little practical concern for several reasons. Significant amount of sea salt is usually present only at sizes larger than the accumulation number mode and sea salt particles generally constitute only a minor fraction of the total particle number greater than 80 nm. When present, sea salt particles usually appear as a separate mode in the hygroscopic growth factor measurements, even if they are associated with small amounts of sulfate through atmospheric processing (Berg et al., 1998b). These particles can be thus be identified and their critical supersaturation can be estimated separately with an appropriate empirical expression for NaCl [e.g. as measured by Tang (1997)]. If there are smaller amounts of NaCl internally mixed with the sulfate particles, the errors introduced into the CCN spectra will be much smaller than 25% depending on the amount of sea salt present. Impactor measurements in Sagres show that sea salt contributed less than 5% of the mass in particles smaller than 250 nm, which provide the majority of the CCN.

2.2.2. Soluble organics. In the approach described in section 2.1 S_c is calculated using equivalent ions that represent all the compounds contributing to the hygroscopic growth at 90% r.h.. Therefore all organic material that is in solution at this r.h. will be represented as an equivalent amount of ions, while the rest is classified as insoluble. For the accurate estimation of S_c, however, it is not the material dissolved at 90% r.h., but the material dissolved at slight supersaturations that is of crucial importance. Thus, the method presented here will be most inaccurate if organic species are present that do not dissolve in the fairly concentrated droplets around 90% r.h. but are able to dissolve when the r.h. nears the critical supersaturation and the droplet is more diluted.

If these soluble compounds were analyzed chemically and their solubilities in sulfate solutions and effects on the surface tension were known their effect could be modeled using a modified Koehler equation (Laaksonen et al., 1998; Shulman et al., 1996; Kulmala et al., 1997). However only a fraction of the organic compounds in the ambient aerosol have been analyzed so far. Dicarboxylic acids are the only compounds whose solubilities in sulfate solutions of various concentrations and whose effect on the surface tension has been measured (Shulman et al., 1996). Those acids are therefore used as model compounds for other soluble organics in the following sensitivity analysis. To estimate errors that could arise in our calculations due to the presence of dicarboxylic acids in the inorganic aerosol particles we compare S_c derived from eqs. (2)–(5) to the critical supersaturation obtained by the more exact treatment using the modified Koehler equation.

Figure 1 demonstrates this comparison for the extreme example of a 60 nm particle that consists of a mixture of 10% ammonium sulfate and 90% organic acid (molar fraction). The dicarboxylic acids considered are: glutaric acid, which is highly soluble, succinic acid, which is moderately soluble, and adipic acid, which is only slightly soluble. Since it is not clear if or how strongly dicarboxylic acids dissociate in solution the modified Koehler curves have been calculated for a Van't Hoff factor i ranging from 1 to 3 and are shown as a shaded area. Also shown are the classical Koehler curves for a 60 nm

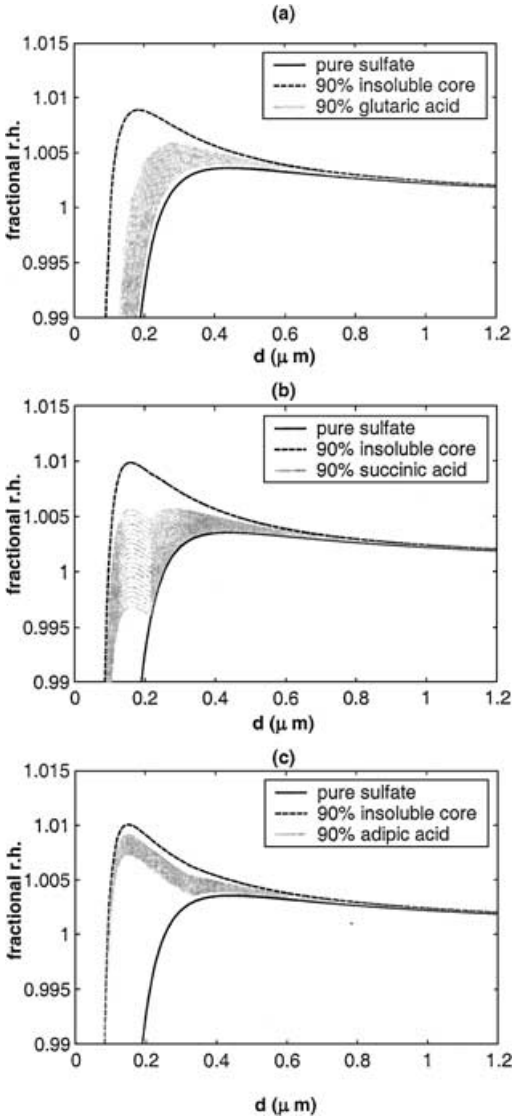

Fig. 1. Modified Koehler curves for 60 nm particles consisting of 10% ammonium sulfate and 90% dicarboxylic acid are shown as shaded areas, taking into account that the Van't Hoff factor of the dicarboxylic acids might vary between 1 and 3. The classical Koehler curves for a particle of pure ammonium sulfate (solid line) and a particle that contains 10% ammonium sulfate and 90% insoluble core are shown for comparison.

particle consisting of pure ammonium sulfate (solid line) and a 60 nm particle that contains an equal volume of insoluble material instead of the organics (dashed line). The first curve represents the Koehler curve that would result from our calculations based on equivalent ions if the organic acid was fully dissolved and fully dissociated at 90% r.h.. The second curve represents the Koehler curve we would result from our calculations if the organic acid was completely insoluble at 90% r.h..

Figure 1a shows the modified Koehler curves for particles containing large amounts of strongly soluble organic material such as glutaric acid. The Koehler curve for the fully dissociated acid (lower boundary of the shaded area) is very close to the solid line representing ammonium sulfate. If an organic acid is mostly dissolved at 90% r.h., it seems justified to approximate its hygroscopic behavior by an equivalent amount of totally soluble, dissociated ions and treat it with the classical Koehler curve.

The hygroscopic behavior of a particle containing a large fraction of a moderately soluble substance cannot be adequately described using hygroscopic growth factors and the classical Koehler theory. Figure 1b shows that at an r.h. below 99% the modified Koehler curve approaches the Koehler curve of a particle with an insoluble core. That means that only a very small fraction of the moderately soluble substance dissolves below 99% r.h and it will not influence the hygroscopic growth at 90% r.h.. The organic acid is therefore interpreted as totally insoluble material when N_i^{eq} are calculated from hygroscopic growth factors at 90% r.h. using eqs. (2)–(5). The calculated critical supersaturation is thus close to the maximum of the dashed line in Fig. 1b representing the Koehler curve of a particle containing an insoluble core. However, this curve deviates strongly from the modified Koehler curve at supersaturations close to S_{c}, and CCN concentrations can be considerably underestimated.

Figure 1c shows the case of a particle containing a slightly soluble substance such as adipic acid. This compound does not dissolve very much at either lower r.h. or at supersaturations close to S_{c}. It will be interpreted as insoluble material in the calculation of N_i^{eq} from hygroscopic growth factors at 90% r.h. and acts as such at supersaturations close to S_{c}. The equivalent ions thus provide a good estimate of S_{c}.

A sensitivity study is conducted for particle sizes from 0.02 to 0.4 μm and for ammonium sulfate particles containing 0–90% dicarboxylic acid by mass. It is assumed that calculations using the modified Koehler equation give the correct S_{c}. Errors in S_{c} estimated by eqs. (2)–(5) are calculated as follows:

The highly soluble glutaric acid is assumed to be fully dissolved and, for simplicity, fully dissociated ($i = 3$) at 90% r.h.. Since for a fully dissolved

substance errors in S_c are independent of the degree of dissociation, this assumption does not influence the results of this analysis. For $i = 3S_c$ estimated based on hygroscopic growth factors is close to the critical supersaturation of a particle consisting of ammonium sulfate S_c^{sulf}, whereas the actual critical supersaturation of the mixed particle is given by the modified Koehler equation (S_c^{mod}). The percentage error in S_c can thus be estimated as $(S_c^{sulf} - S_c^{mod})/S_c^{mod} \times 100$.

Succinic and adipic acid are presumably not dissolved at 90% r.h.. S_c calculated based on hygroscopic growth factors is close to the critical supersaturation of a particle containing insoluble material instead of an organic acid S_c^{ins}. A Van't Hoff factors ($i = 2$) is assumed for these calculations. The percentage error in S_c can thus be calculated as $(S_c^{ins} - S_c^{mod})/S_c^{mod} \times 100$.

The percentage errors are shown in Fig. 2 for particles consisting of ammonium sulfate and glutaric acid (a), succinic acid (b) and adipic acid (c). Errors for particles consisting of glutaric acid and ammonium sulfate are generally negative, i.e. the critical supersaturation of such particles is underestimated by the calculations. These errors are mostly due to effects of glutaric acid on the surface tension of the droplet near critical supersaturations. The magnitude of these errors is <10% for organic mass fractions <0.9 and is not expected to affect the calculated CCN concentrations strongly. The critical supersaturations for ammonium sulfate particles containing succinic and adipic acid are overestimated and the errors are much larger than for particles containing glutaric acid. The errors are mostly caused by the fact that only a negligible part of these dicarboxylic acids is in solution at 90%, but they dissolve to a larger extent near the critical supersaturation. In this case changes in surface tension are only second order effects. For adipic acid the errors in S_c are smaller than 30%, at organic mass fractions less than 60%. For succinic acid the errors are smaller than 30% at organic mass fractions less than 50%.

Assuming that dicarboxylic acids are appropriate as model compounds for other soluble organic species the sensitivity studies indicate the errors in the calculations will not be too large unless large quantities (larger than 50% by mass) of slightly or moderately soluble material such as succinic or adipic acid are present in the aerosol. Considering that about 30–70% of the organic material in the atmospheric aerosol is insoluble (e.g. Saxena and Hildemann, 1996) this corresponds

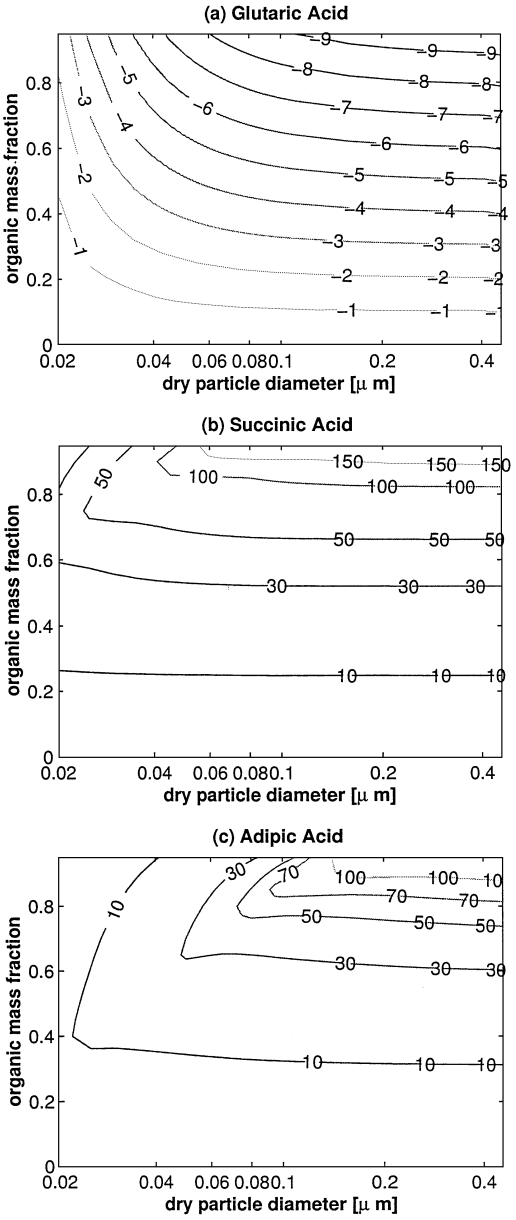

Fig. 2. Deviation of the critical supersaturation calculated using classical Koehler theory and hygroscopic growth factors from the values of S_c obtained by the full calculations based on the modified Koehler theory. The deviations are shown in as percentages for a range of particle sizes and organic mass fractions. Negative values indicate an underestimate of S_c by the classical Koehler theory, positive values indicate an overestimate.

to an organic mass fraction of at least 80%. Such high concentrations of organics are not very common in the atmosphere, but can be found in aerosols from forest fires in South America or Africa (Yamasoe et al., 2000; Andreae et al., 1998).

During the ACE-2 field experiment submicron mass fractions of total carbon were on average about 15% at the Sagres site. Even if all this carbon was slightly soluble, which is highly unrealistic, the resulting errors in S_c still would be below 10%. The sensitivity study indicates that during ACE-2 not enough organic material is present at Sagres to introduce significant errors into our calculation by the 'dissolution effect' of slightly soluble organics.

2.2.3. Other effects. Some of the effects that might cause the calculated CCN concentration to be inaccurate are not known well enough to be included in a systematic sensitivity study. It has sometimes been proposed that certain organic species might inhibit or slow down the particle water uptake. If such compounds were present in atmospheric aerosol the CCN concentrations would be overestimated by the calculations in section 2.1. However, little is known about the occurrence of such substances in the ambient atmosphere. Some laboratory studies indicate that even thick coatings of water insoluble materials (DOP) cannot inhibit CCN formation (Cruz and Pandis, 1998).

Some surfactant organic species might have a stronger effect on the surface tension and affect the calculation of effective ions or the the critical supersaturations much more strongly than dicarboxylic acids. A sensitivity study showed that the calculated number of equivalent ions is not very sensitive to the surface tension at 90% r.h. For a 50% decrease in surface tension, an extreme value, the change in calculated effective ions was less than 5%. At or near critical supersaturation, the equilibrium size of the particle is more strongly dependent on the surface tension. If the surface tension of the droplet decreases by 10% due to surfactant species, CCN concentrations could be underestimated by the calculations by up to 30%. Strongly surfactant compounds could thus potentially introduce large errors in the estimated CCN spectra. However, the surface tension of cloud water sampled in Tenerife during ACE-2 did not differ significantly from that of pure water Faccini et al. (2000). Since the concentration of organic species in Sagres during ACE-2 is low, organics will probably have a small effect on CCN activation at this location even when the droplets are more concentrated at relative humidities near critical supersaturation.

Moreover, the uptake of soluble gases into the growing droplets could decrease S_c significantly. The uptake of soluble gases into concentrated solution droplets is difficult to estimate since it depends on the composition, concentration and pH of the solution. The uptake of soluble gases would lead to an underestimate of CCN concentrations by the calculations. For this study, it is impossible to estimate the magnitude of this effect because of lack of air chemistry and thermodynamic data.

Despite these possible shortcomings it can be useful to the calculate CCN spectra in situations where the organic mass fractions are low. Both the hygroscopic growth factor and the aerosol size distributions can be measured using established, calibrated techniques at high size and temporal resolution. Using simple and tried measurement methods combined with calculations even if some assumptions have to be made can be an advantage to more complicated instruments that are susceptible to larger measurement uncertainties. In the following section one crucial assumption is tested against measurements to assure that it does not introduce significant errors into the CCN calculations.

3. Hygroscopic consistency study

The calculation of CCN based on hygroscopic growth factors involves the crucial step of estimating the number of equivalent ions in the aerosol particles which are representative of all hygroscopic and soluble species that contribute to the hygroscopic growth at 90% r.h.. If the aerosol does not contain much soluble organic material the number of equivalent ions based on hygroscopic growth factors should be comparable to the number of chemically analyzed inorganic ions in the particle. At Sagres, where the aerosol was mainly composed of ammonium and sulfate (on average more than 80% of the submicron mass), such a comparison is possible. Thus, a comparison of the number concentrations of equivalent ions calculated using hygroscopic growth factors and particle number size distribution to the number concentrations of inorganic ions found by the chemical analysis of impactor samples can be made. Similar studies have been done previously by Swietlicki et al. (1999) and Berg et al. (1998a). If this internal consistency study is successful it gives confidence in the impactor and growth factor measurements and also in our ability to derive inorganic ions from growth factor measurements.

3.1. Data base

The data necessary for the hygroscopic consistency study are: the number concentration of inorganic ions chemically analyzed in impactor samples, the particle number size distributions from 50 to 800 nm, and hygroscopic growth factors to calculate the numbers of equivalent ions in a single aerosol particle. The latter two measurements can be combined to estimate the number concentration of equivalent ions in certain particle size ranges. During the ACE-2 measurement campaign in Sagres aerosol particles were sampled using a Berner type, low-pressure impactor (Berner and Lürzer, 1980). The impactor collected aerosol in five stages with d_{50} cut-offs at 0.05, 0.14, 0.42, 1.2, 3.5 and 10 μm aerodynamic diameter (d_{ae}) at a controlled humidity of 60% r.h.. The deposits were extracted in deionized water and analyzed by capillary zone electrophoresis. Organic and elemental carbon were determined by a thermal desorption method. The experimental methods and the chemical data are described in more detail in Neusüß et al. (2000). The hygroscopic growth factors of particles with dry diameters of 35, 50, 100, 150 and 250 nm were measured using a TDMA (Swietlicki et al., 2000). Number size distributions were measured by a high-resolution Twin Differential Mobility Analyzer (TDMPS) (Birmili et al., 1999) in the size range from 3 to 800 nm.

This consistency test is done for the second impactor stage that collects particles with d_{ae} between 0.14 and 0.42 μm. The aerodynamic cut-off sizes of impactor stage 2 refer to particle sizes at the impactor sampling r.h. of 60% ($d_{\mathrm{ae}}^{60\%}$), where the particles are probably still hydrated due to hysteresis effects and the occurrence of hygroscopic salts with low deliquescence humidities such as ammonium bisulfate. In the TDMPS and TDMA system the aerosol particles are dried to an r.h. of $<10\%$ before the measurements are made. Therefore the impactor cut-offs have to be converted to dry Stokes diameters (d^{dry}) to be comparable to the TDMA and TDMPS measurements:

$$d^{\mathrm{dry}} = \frac{1}{G^{60\%}}\sqrt{\frac{C_{\mathrm{c}}\left(d_{\mathrm{ae}}^{60\%}\right)}{C_{\mathrm{c}}(d^{60\%})\rho^{60\%}}}\,d_{\mathrm{ae}}^{60\%} = \sqrt{\frac{C_{\mathrm{c}}\left(d_{\mathrm{ae}}^{60\%}\right)G^{60\%}}{C_{\mathrm{c}}(d^{60\%})\left(\rho_{\mathrm{dry}} + [(G^{60\%})^3 - 1]\rho_w\right)}}\,d_{\mathrm{ae}}^{60\%} \tag{6}$$

where ρ_{dry} is the density of the dry aerosol particles, $\rho^{60\%}$ the density of the aerosol particles at 60% r.h., ρ_{w} the density of water, and $G^{60\%}$ the hygroscopic growth factor of the particles at 60% r.h. and C_{c} is the Cunningham slip correction factor. Using eq. (6) the lower and upper cut-off diameters of impactor stage 2 are converted to dry Stokes diameters of 0.09 and 0.29 μm, respectively. Campaign averages of the growth factors at 60% (1.21 at 0.09 μm and 1.25 at 0.29 μm) and a dry density of 1.6 g cm^{-3} were used.

3.2. Calculation procedure

The concentration of equivalent ions for particles in the size interval between 0.09 and 0.29 μm is estimated from hygroscopic growth factors and the number size distribution. The hygroscopic growth factors at 100, 150 and 250 nm are interpolated to the diameters of size distribution measurements. The growth factor is expected to be a smooth function of diameter, since it is dependent on chemical composition, and chemical analysis with a factor of two size resolution shows continuity. Our understanding of physical and chemical processing of atmospheric aerosol supports this expectation of continuity of G with size for these size increments. At those diameters the equivalent number of ions per particle N_i is calculated as described in section 2.1 using eq. (2)–(5). Aerosol collected on impactor stage 2 consists almost exclusively of ammonium and sulfate. The measured ammonium to sulfate ratio R of each impactor sample is used to decide if ammonium sulfate [$(NH_4)_2SO_4$, $R > 1.75$], letovicite [$(NH_4)_3H(SO_4)_2$, $1.25 < R < 1.75$] or ammonium bisulfate (NH_4HSO_4, $R < 1.25$) is the dominant sulfate compound. For ammonium sulfate and letovicite an appropriate empirical expression similar to eq. (4) is used in the calculation. The empirical expressions are based on measured data by Tang and Munkelwitz (1994).

The growth factor measurements indicate that sometimes the aerosol at Sagres consists of an external mixture of more hygroscopic and less hygroscopic particles. For those external mixtures N_i values are calculated separately for the more hygroscopic particles (N_i^{mh}) and the less hygroscopic particles (N_i^{lh}). The number concentration of equivalent ions $\mathrm{d}N_i/\mathrm{d}\log d$ at each diameter d_k of the size distribution measurements are calculated as follows:

$$\frac{\mathrm{d}N_i}{\mathrm{d}\log d_k} = N_i^{\mathrm{mh}}(d_k)\frac{\mathrm{d}N}{\mathrm{d}\log d_k}n_{\mathrm{mh}}(d_k) + N_i^{\mathrm{lh}}(d_k)\frac{\mathrm{d}N}{\mathrm{d}\log d_k}n_{\mathrm{lh}}(d_k) \tag{7}$$

where $dN/d\log d_k$ is the number size distribution at diameter d_k and $n_{mh}(d_k)$ and $n_{lh}(d_k)$ are the relative number fraction of more and less hygroscopic particles at diameter d_k.

The number concentration of ions at the seven diameters d_k that lie within the size interval between the cut-off diameters of impactor stage 2 are averaged. Since the impactor sampling time is much longer than the time for a TDMPS measurement, equivalent ions are calculated for each TDMPS measurement during one impactor run and subsequently averaged. Samples for which less than 50% of the impactor run time is covered by DMPS and TDMA measurement are excluded from the analysis.

3.3. Results

The number concentration of inorganic ions as measured by chemical analysis of the deposits on impactor stage 2 vs. the number concentration of equivalent ions calculated from hygroscopic growth factors is shown in Fig. 3 along with uncertainty estimates described below. Most of the data points lie close to the 1:1 line. Since the data points have uncertainties both in the x and y direction the reduced major axis regression (RMA) was used to fit a straight line to the data (Ayers, 2001). Unlike the conventional linear regression the RMA method yields a fit line that is invariant to exchanging the x and y axes. The resulting linear fit ($dN_i^{est}/d\log d = k\, dN_i^{meas}/d\log d + d$) yields $k = 0.91$ and $d = 11$ with $R^2 = 0.9$.

On average the ratio of calculated ion number concentrations to the measured ones is 1.11 ± 0.28. This overestimate by 11% is mostly due to a difference in measured and calculated ion number concentrations in clean conditions. It can be seen that the measured values are significantly lower than the calculated values at very low aerosol concentrations. If the seven data points with ion number concentrations lower than 40 nmol m^{-3} are excluded, the average ratio of calculated to measured ions decreases to 1.03 ± 0.21.

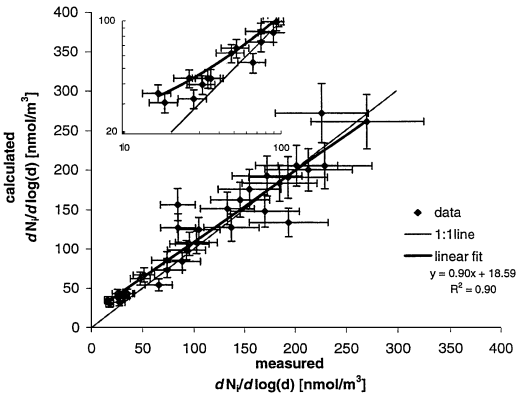

Fig. 3. Comparison of the measured and the calculated ion number concentrations for impactor stage 2. The inset shows the data below 100 nmol m^{-3} on a logarithmic scale.

The consistency test can be considered successful if the differences in measured and calculated ion number concentrations can be explained by the measurement uncertainties. The consideration of the uncertainties in both measurements and calculations is thus an important part of a consistency test [see e.g. Quinn et al. (1996)]. The uncertainties in the chemical analysis, particle number concentrations and growth factors are estimated based on the 1σ standard deviation of repeated measurements, calibrations and counting statistics.

The 1σ uncertainty in number concentration of ions determined by the chemical analysis is roughly $\pm 20\%$ [Neusüß et al. (2000)]. The experimental uncertainty of the hygroscopic growth factors at 90% r.h. is estimated to be $\pm 5\%$ due to sizing, flow and counting statistics in the TDMA system. Also the uncertainty in the fraction of more hygroscopic and less hygroscopic particles is approximately $\pm 5\%$, arising mostly from inaccuracies in the fitting routine. The particle number concentration is known to approximately $\pm 10\%$, and sizing errors of the TDMPS and TDMA system lead to an uncertainty in dry particle size of about $\pm 1\%$.

The uncertainties in particle number concentrations and growth factor have to be propagated through the ion concentration calculation. A Monte Carlo approach is used for the error propagation. The input parameters (the more and less hygroscopic growth factors G^{mh} and G^{lh}, the fraction of more hygroscopic particles n_{mh}, the particle diameter d and the particle number concentration $dN/d\log d$ are each randomly generated assuming that they are normally distributed around the measured value with a standard deviation of the measurement uncertainty. Then the number concentration of equivalent ions is calculated. This procedure is repeated 10 000 times and the mean and the standard deviation of the resulting 10 000 ion number concentrations are calculated. The standard deviation of the Monte Carlo results represents the uncertainty in the ion number concentrations arising from the measurement uncertainties. These uncertainties are averaged over the impactor size interval and measurement times.

The uncertainties in calculations and measurements are shown as uncertainty bars about the data points in Fig. 3. These uncertainty bars represent 1 standard deviation, i.e. a probability of 68% that the 'true' ion concentration lies between those uncertainty bars. It follows that including uncertainty bars 68% or more of the data points must lie on the 1:1 line if the difference in calculated and measured ions is due to measurement uncertainties alone. In this experiment approximately 75% of the data include the 1:1 line within their uncertainty bars. This shows that the calculated and measured ion number concentrations agree within the measurement uncertainties and that the calculations and measurements are consistent within our experimental uncertainty.

3.4. Discussion

The results of the hygroscopic consistency study show that in the presence of low concentrations of organic material as observed in Sagres and generally during ACE-2 (Neusüß et al., 2000; Putaud et al., 2000) the calculated equivalent ion concentrations reproduce the measured number concentrations of inorganic ions successfully. This suggests that the hygroscopic growth factor measurements are valid and that it is possible to use those measurements for predicting the number of ions in a particle.

On average the calculated ion number concentrations are 11% greater than the chemically measured ion number concentration. At low number concentrations (clean conditions) this difference is significant. This is an indication that the particle water uptake at 90% r.h. is higher than that attributed to the measured inorganic ions alone implying that other species such as soluble organics could have contributed to the hygroscopic growth. However, there is no indication that the particle water uptake not explained by inorganic ions increases when the mass fraction of organic compounds in Sagres is high. In fact these two quantities are completely uncorrelated. Thus there is no indication that organics contribute to the hygroscopic growth even in clean conditions when the organic mass fractions are higher. It is more likely that in clean conditions the detection level of the impactor measurements is approached. Systematic errors in the chemical analysis at those low sample amounts are most likely the explanation for the differences between measurements and calculations at low ion number concentrations.

4. CCN spectra in Sagres during ACE-2

Direct measurements of CCN spectra during ACE-2 in Sagres are limited to a few days. One objective of this work is to compare calculated and measured CCN spectra. Another more general objective is to calculate a larger data set of CCN spectra based on hygroscopic growth factors and number size distributions to be able to compare CCN spectra representative of different air masses and air mass histories that occurred during ACE-2. The number size distribution measured by the TDMPS system and growth factors measured by the TDMA are used in the calculations. For all particles in the size distributions the critical supersaturation S_c is estimated as described in section 1 using eqs. (1)–(5). The ammonium to sulfate ratios of impactor samples were used to identify the dominant sulfate salt and an appropriate empirical expression for each salt was used as eq. 4. The number concentration of particles activated at supersaturation S is calculated as the sum over all particles with $S_c < S$. Experimental uncertainties in the measurements of hygroscopic growth factors, particle diameters and number concentrations are propagated to CCN concentrations using a Monte Carlo method analogous to the one described in section 3. CCN spectra are calculated for all time periods in the ACE-2 field campaign in Sagres for which size distribution and growth factor measurements are available.

4.1. Comparison of calculated and measured CCN spectra

CCN spectra were measured using a CCN remover (CCNR) (Ji et al., 1998). In this instrument number size distributions are measured downstream of a supersaturation chamber, where S is varied from 0% to approximately 1% and nucleated particles are removed by gravitational settling. After passing the supersaturation chamber the particles are dried and their size distributions are measured by an electrical mobility analyzer. The difference between the number concentration of particles measured at $S = 0\%$, the reference size distribution, and the number concentration at a higher S yields the number concentration of CCN.

During the experiment at Sagres, 12 sets of CCNR measurements were made that could be compared to the TDMPS and hygroscopic growth data. As a first step, each of the CCNR reference size distributions ($S \leq 0\%$) was compared to the DMPS size

distributions for the same measurement time interval to determine the counting efficiency of the CCNR DMA cf. the TDMPS, i.e. the ratio of dN/d log d for the CCNR to dN/d log d for the TDMPS. Since the TDMPS size distributions have been validated in various comparisons [e.g. the hygroscopic consistency study in the previous chapter, a closure study involving impactor mass (Neusüß et al., 2000)], and a comparison of total number with a condensational particle counter, they can serve as a standard against which the more indirectly measured CCNR size distribution can be evaluated.

The average CCNR counting efficiency of the 12 sets of measurements is shown in Fig. 4a. The counting efficiency changed from measurement to measurement, but for any given measurement it was approximately constant between 50 to 200 nm and was less for larger and smaller sizes. The fact that the plateau region between 50 and 200 nm is much smaller than 1 is due to a dilution inherent in the operation of the CCNR (Ji et al., 1998). The dilution factor is highly sensitive to the balance of four major flows in the CCNR and varied during the experiment from 6 to 12. Combined errors of ±5% in these measured flows lead to uncertainties of a factor of ±50% in the minor, inlet flow to the system. Therefore, the dilution factor derived from flow measurements has large uncertainties. In this work we derive the individual dilution factors for each CCNR measurement using the CCNR counting efficiency. For each individual measurement the dilution factor is defined as the factor necessary to shift the plateau region of the counting efficiency to 1.

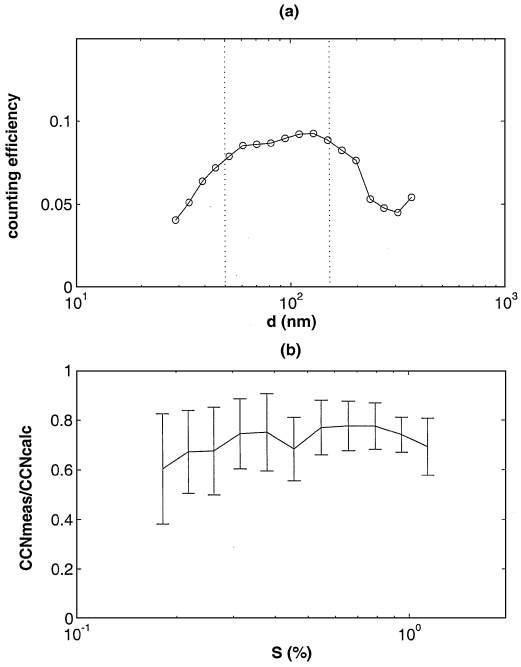

Fig. 4. (a) The average counting efficiency of the CCNR instrument cf. the TDMPS instrument for the 12 measurements used in this comparison. Particle diameters of 50 and 150 nm are indicated by dotted vertical lines. The shift of the plateau region from 1 is due to a dilution inherent in the operation of the CCNR. (b) The average ratio of measured to calculated CCN after the dilution factors of the CCNR instrument have been taken into account.

The size-dependent variation of the CCNR efficiency in comparison with the TDMPS is not due to dilution effects. It may be a result of the fact that the two systems used different inlet line lengths, different DMAs and different scanning programs and inversion routines. The additional 2 m inlet line leading to the CCNR would have contributed to losses of smaller particles due to diffusion, but these diffusion losses should be less than 10% at 40 nm. The TDMPS was a HAUKE unit operating with a size stepping scan and an inversion routine from IfT. The CCNR DMA was a TSI unit operating in a continuously scanning mode with the TSI SMPS inversion software. The loss of particles larger than 150–200 nm can be explained by the fact that the CCNR reference size distributions are measured after the aerosol passed the supersaturation chamber at $S = 0\%$. At these high relative humidities some of these particles can take up sufficient water due to simple hygroscopic growth that they fall out of the air stream as if they were cloud droplets and are not counted. Data outside the range 50–200 nm do not materially affect our results or apply to atmospheric CCN because we have restricted our discussion to supersaturations less than 1% and because particles greater than 200 nm contributed a small fraction of the CCN.

Figure 4b shows a comparison of the calculated and CCNR measured CCN spectra after the dilution inherent in the CCNR instrument was taken into account. Average values for the 11 measurements are shown along with error bars representative of 95% confidence limits. The larger range at small supersaturations is mostly due to noise in the CCNR instrument at low particle count.

The results of the comparison for each CCNR measurement are presented in Fig. 5 at selected supersaturations. The calculated and measured CCN number concentrations at $S = 0.3\%, 0.5\%, 0.7\%$ and 0.9% are plotted in Figs. 5a–d along with the least-square best

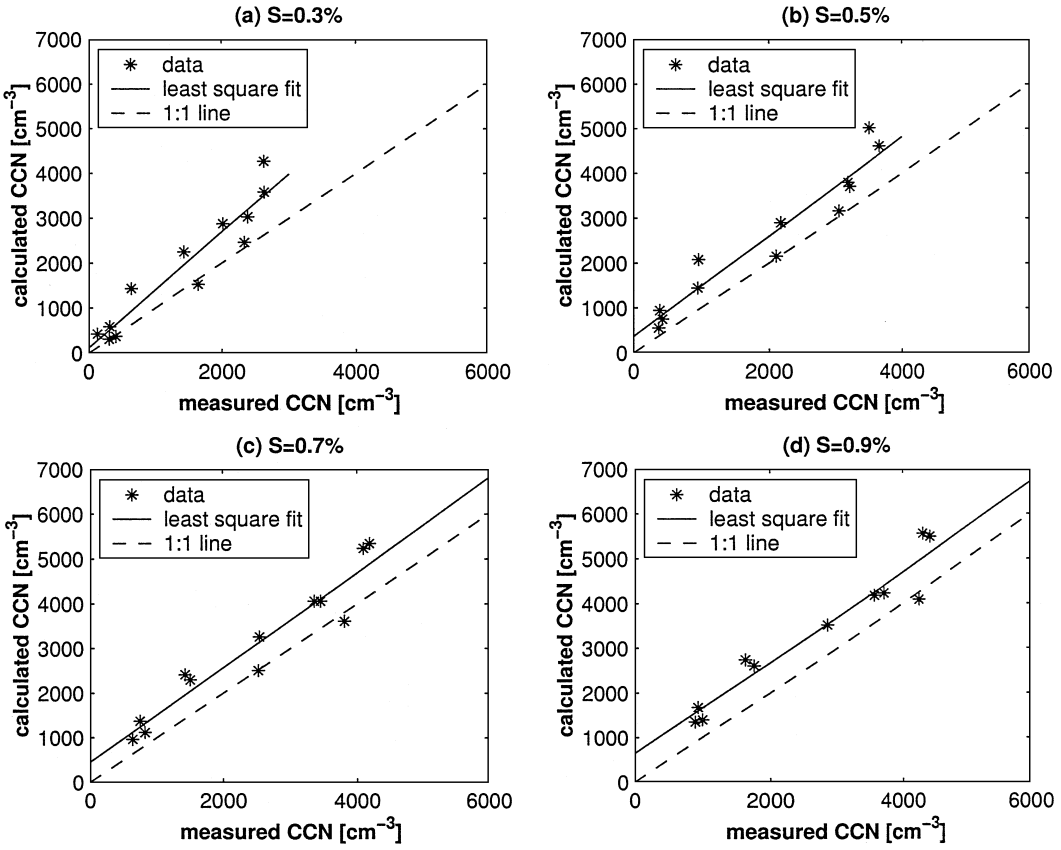

Fig. 5. Calculated vs. measured CCN concentrations at different supersaturations. Also shown are the 1:1 line and linear least-square fits for each case.

fit (solid line) and the 1:1 line (dotted line). The results for the slope and residual of the linear regression lines ($[\mathrm{CCN}]_{\mathrm{calc}} = k[\mathrm{CCN}]_{\mathrm{meas}} + d$) are given in Table 1. The R^2 values are generally high, between 0.89 and 0.93. The calculated CCN concentrations still seem to be larger than the measured CCN concentrations. The measurements and calculations differ on average by $35 \pm 20\%$ at $S = 0.3\%$, $34 \pm 14\%$ at $S = 0.5\%$, $27 \pm 10\%$ at $S = 0.7\%$ and $28 \pm 10\%$ at $S = 0.9\%$. The difference is significant at the 95% confidence level in all cases. However, it should be noted that at $S = 0.3\%$ the mean difference between measurements and calculations is of the same order of magnitude as the measurement uncertainties.

Table 1. *Slopes (*k*) and residuals (*d*) for the linear least squares fits shown in Fig. 4, with the corresponding 95% confidence intervals (CI)*

S (%)	k	95% CI	d (cm^{-3})	95% CI	R^2
0.3	1.29	0.98–1.59	116	−403–635	0.89
0.5	1.12	0.89–1.33	367	−150–885	0.93
0.7	1.06	0.84–1.28	447	−150–1045	0.92
0.9	1.01	0.81–1.21	643	24–1261	0.93

The overestimate could have different reasons. After the dilution correction there are still some differences in the base size distributions, for example due to the selective loss of large particles in the CCNR as explained above. These second-order differences in the base size distributions could explain some of the discrepancy between measured and calculated CCN spectra, but surely not all of it. Another possible reason is that some of the aerosol particles might contain organic species that inhibit or slow down the water uptake. In this case particles that are technically

activated at the supersaturation in the CCNR might grow too slowly to fall out of the air stream in the instrument. There have been indications that the Van't Hoff factor of ammonium sulfate might be lower than 3 in droplets of sizes near the critical radius. If the Van't Hoff factor was decreased by 30% in the growing droplets the assumption that the inorganic species are fully dissociated could introduce an error that varies from 20% to 10% for supersaturations from 0.3% to 1%.

Finally kinetic limitations could prevent the activation of some particles in the instrument. It has been proposed that this process might influence the CCN concentrations in stratus clouds (Chuang et al., 1997; Nenes et al., 2001). However, due to the long residence time of the particles in the CCNR (greater than 1 min) this effect is very unlikely. Thus the difference between measurements and calculations cannot be explained with certainty, especially since the hygroscopic consistency study showed agreement between measured ion number concentrations and equivalent ions derived from growth factor measurements. However, it is also important to keep in mind that there are few data points in this comparison and the 95% confidence levels on both the slopes and the residuals are quite large. The results should thus not be over interpreted.

The fact that the calculated CCN concentrations are larger than the measured ones suggests that in Sagres neither soluble gases nor moderately soluble or surfactant organic compounds have a strong influence on the instrumental CCN activation. Surfactant organic species, slightly soluble organics and soluble gases all decrease the critical supersaturation (S_c). If any of those effects were significant in Sagres the calculated CCN concentrations would be lower than the measured concentrations. It might also be possible that these effects are present but their influence on the critical supersaturation is accounted for by the estimation of equivalent ions from hygroscopic growth factors.

In other recent studies (Chuang et al., 2000; Wood et al., 2000; Snider and Brenguier, 2000) the differences between measured and calculated CCN concentrations are larger than in this work and are in extreme cases as large as a factor of 5. In this context the comparison presented here seems to be reasonably successful after the dilution correction has been applied. There is a strong similarity in the shape of the calculated and measured CCN spectra and calculated and measured CCN concentrations are strongly correlated. It seems thus useful to complement the limited number of measured CCN spectra with a larger, calculated data set that covers most of the ACE-2 period in Sagres, bearing in mind that CCN concentrations might be somewhat overestimated.

4.2. Calculated CCN spectra in different air mass conditions

During the ACE-2 field experiment the measurement site at Sagres was influenced by several different air mass types. For the first half of the experiment clean air coming from the Atlantic prevailed, whereas during the second half polluted air masses originating over the European continent reached Sagres more frequently. The whole data set of CCN spectra is subdivided into clean and polluted time periods according to air mass back trajectories. Trajectories for the clean time periods originate over the Atlantic or the Arctic ocean. In many cases, air masses reach the Iberian Peninsula to the north of Sagres and flow down the coast to the Sagres measurement site. Those cases are eliminated from the marine data set to avoid contamination from local sources along the coast. Trajectories for the polluted time periods are subdivided according to the distance, time and pathway from the source region. Air masses containing aged pollution originate over France or Great Britain and flow out over the Atlantic, where they spend several days before reaching Sagres. Air masses containing more recent pollution originate over central Europe or the Mediterranean region and cross the Iberian Peninsula before they reach Sagres from inland. Examples of back trajectories for the three air mass types are shown in Fig. 6.

Figure 7a shows a comparison of average CCN spectra in clean conditions, aged and fresh pollution. The

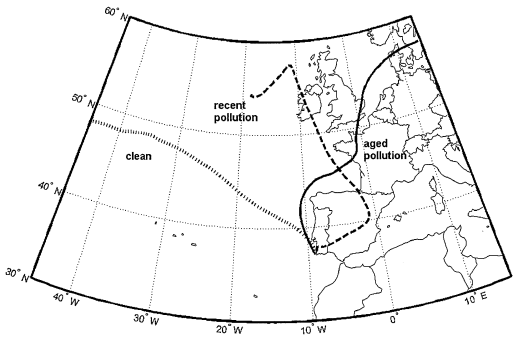

Fig. 6. Typical air mass back trajectories for time periods during which Sagres was influenced by clean air masses (dotted line), by aged pollution (solid line) and by recent pollution (dashed line).

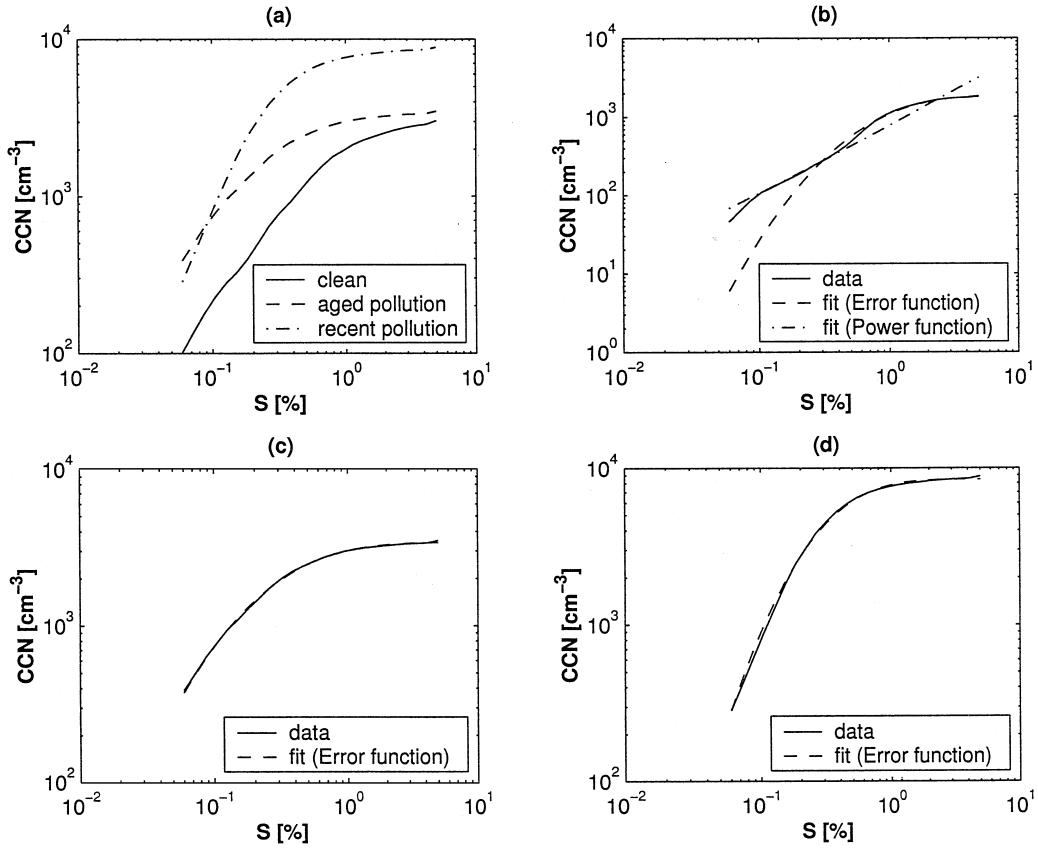

Fig. 7. (a) Calculated CCN spectra averaged over all clean time periods (solid line) and over the time periods when Sagres received aged pollution (dashed line) and recent pollution (dash-dotted line). (b) The CCN spectrum for clean conditions (same as in Fig. 7a) is shown along with a fitted error function (dashed line) and a fitted power function. (c) The average CCN spectrum in aged pollution (solid line) together with the best fit Error function (dotted line, mostly invisible because it coincides with the measured spectrum). (d) same as in (c) but for recent pollution.

spectra in polluted air are similar at low supersaturations (S), but at $S > 0.1\%$ the CCN concentrations in the recently polluted air mass exceed the CCN concentration in aged pollution by a factor of up to 3. This result agrees with observations that recently polluted air masses contain more newly formed particles and the aerosol size distribution is shifted towards smaller particles. These small particles are activated at higher supersaturations, resulting in CCN spectra that increase strongly at higher S. In the aged pollution those fine particles have mostly vanished due to coagulation and growth processes. At the same time the number of larger particles in the air mass contaminated by aged pollution increases so that at low S the CCN spectra in aged pollution are comparable to the ones in fresh pollution. The clean air masses are comparatively devoid of large particles that activate at low supersaturations, but the CCN spectra in clean conditions and aged pollution are similar at $S > 1\%$.

The CCN that are activated at supersaturations typical for stratus clouds are most important in the indirect effect of aerosols on climate. Those supersaturations are generally estimated to lie below 0.5% (e.g. Cantrell et al., 1999; Vong and Covert, 1998). CCN activated at those low supersaturations are increased strongly by pollution. The CCN concentrations at $S = 0.2\%$ are on the average 400–500 cm^{-3} in clean conditions and increase to approximately 1500 cm^{-3} in aged pollution and to 2500 cm^{-3} in recent pollution. Even aged pollution in air masses that spent several days over the ocean has a large effect on the CCN concentrations at supersaturations typical for stratus clouds.

Similarly high cloud droplet number concentrations have been measured in a cap cloud in Tenerife during the ACE-2 measurement period when polluted air masses reached the island after days of transport over the ocean (Martinsson et al., 2000).

4.3. Parameterization of CCN spectra based on lognormal size distributions

The CCN spectra in different air mass conditions can be parameterized for modeling purposes. Traditionally a power function of the form $S = CS^k$ has been used for that purpose (e.g. Twomey, 1959; Hudson et al., 1998). However, there is no physical reason why the CCN spectra should follow a power law. This has also been noted by Ji and Shaw (1998), who propose an exponential function for the description of CCN spectra. It is well established that the size distribution of the atmospheric aerosol within the Aitken and accumulation mode range can be described by one or a combination of two or more lognormal distributions. Since a CCN spectrum is to a first approximation an integration of the size distribution, the CCN spectra should have the form of an error function (erf). In this work we thus chose the following function for the parameterization of the CCN spectra:

$$N_{\mathrm{ccn}} = A\left[1 + \mathrm{erf}\left(\frac{-\log(S) + B}{C}\right)\right], \tag{8}$$

with A, B and C as adjustable parameters.

The error function proposed in eq. (8) was fitted to the three average CCN spectra in Fig. 7(a). The parameters A, B and C for each spectrum are summarized in Table 2. The fitted curves are shown as the dashed lines along with the CCN spectra (solid lines) in Figs. 7b–d for the three different air mass conditions. A single error function proposed in eq. (8) provides an almost perfect fit for the CCN spectra in polluted conditions. These spectra clearly do not follow the traditional power function, which would appear as a straight line on a log–log plot. Instead the spectra become sub-linear near supersaturations of about 0.3%, consistent with a lognormal particle size distribution. However, the error function proposed in eq. (8) does not provide a good fit for the average CCN spectrum in clean conditions. The CCN at low S are seriously underestimated as can be seen in Fig. 7b. This discrepancy arises because the particle size distributions in clean marine conditions are generally bimodal and cannot be approximated by a single lognormal distribution. Indeed the CCN spectra of aerosol with a bimodal size distribution appear roughly linear in the log–log plot. The power function is therefore a better approximation for the clean CCN spectra than a single error function, although it is not theoretically linked to the particle size distribution. The power function is useful to approximate marine CCN spectra, but our results show that it cannot be simply extrapolated to polluted conditions. A better approximation for the clean CCN spectra is, however, achieved by using a linear combination of two error functions:

$$N_{\mathrm{ccn}} = A_1\{1 + \mathrm{erf}[-\log(\mathrm{S}) + B_1]\} + A_2(1 + \mathrm{erf}[-\log(S) + B_2]), \tag{9}$$

where the parameter C has been set to 1, to avoid too many free parameters. The values of the parameters can be found in the lower part of Table 2. The fit (not shown in Fig. 7b) is not visually distinguishable from the measured spectrum.

Table 2. *Error function fit parameters for different air mass conditions*

Air mass	A (cm^{-3})	B	C
Clean	940	0.2	1.4
Aged pollution	1700	1.4	1.6
Recent pollution	4240	1.2	1.2
Clean (two error functions)	86 805	2.4 0.1	– –

5. Summary and conclusions

In this paper we proposed a method of calculating CCN spectra from measured number size distributions and particle hygroscopic growth factors. The hygroscopic growth factors are used to derive equivalent ions and equilibrium droplet growth and subsequently the critical supersaturation (S_c). Errors can be introduced into the calculations if the aerosol contains very high fractions of moderately soluble organic species, by the uptake of soluble gases into the growing droplet and by the presence of surface active organic compounds. In those cases the CCN concentrations would be underestimated. However, in Sagres the calculated CCN concentrations are larger than the measured ones. Therefore it can be concluded that organic species and dissolution of soluble gases did not have a strong influence on the CCN activation at this location.

The method of estimating equivalent ions from hygroscopic growth factors was independently tested by an internal hygroscopic consistency study. The number concentration of calculated equivalent ions was compared to the number concentration of ions obtained from chemical analysis of impactor samples. Measured and calculated ions agree within the respective uncertainties except for samples taken on days with low particle number concentrations. In those very clean conditions the calculated ion concentrations are substantially higher than the measured concentrations and it is likely that the detection level of the impactor/chemical analysis method is reached.

CCN spectra were calculated throughout the ACE-2 measurement period whenever size distribution and growth factor measurements were available. The spectra were averaged over time periods when Sagres received clean North Atlantic air masses and air masses influenced by aged or recent pollution from continental Europe. CCN concentrations at supersaturations typical for stratus clouds are strongly enhanced by pollution outbreaks compared to CCN concentrations in marine background conditions. Even in air masses that contain aged continental pollution and spent several days over the Atlantic before reaching Sagres the CCN concentrations at $S = 0.2\%$ are about three times higher than in clean air masses. In recent pollution when air masses reach Sagres from inland or the Mediterranean sea the CCN concentrations are about five times higher than in clean air masses.

In polluted air masses the shape of the CCN spectra changes. The clean spectra can be described by the power function often used in the literature, although this function is not physically linked to the particle size distribution. This power function is only a good approximation to the clean CCN spectra if the size distribution is bimodal in marine background air masses. When continentally polluted air masses reach Sagres the number size distribution resembles a unimodal lognormal distribution. In those polluted cases an error function provides a very good fit to the data.

6. Acknowledgements

This research is a contribution to the International Global Atmospheric Chemistry (IGAC) Core Project of the International Geosphere–Biosphere Programme (IGBP) and is part of the IGAC Aerosol characterization Experiments (ACE). Financial support for the measurements and analyses by the University of Washington was provided by the US National Science Foundation ATM 9619984. This publication was supported by the Joint Institute for the Study of the Atmosphere and Ocean (JISAO) under NOAA Cooperative Agreement #NA67RJ0155, Contribution #845. The CCNR measurements, conducted by the University of Alaska Fairbanks, were funded by the US National Science Foundation, Atmospheric Chemistry, Award 9619488. The authors thank two anonymous reviewers for valuable comments on the manuscript.

REFERENCES

Andreae, M. O., Andreae, T. W., Annegarn, H., Beer, J., Cachier, H., le Canut, P., Elbert, W., Maenhaut, W., Salma, I., Wienhold, F. G. and Zenker, T. 1998. Chemical composition of aerosol emissions from savanna fires in southern Africa: 2. Aerosol chemical composition. *J. Geophys. Res.* **103**, D24, 32119–32128.

Ayers, G. P. 2001. Comment on regression analysis of air quality data. *Atmos. Environ.* **35**, 2423–2425.

Berg, O. H., Swietlicki, E., Frank, G., Martinsson, B. G., Cederfelt, S.-I., Laj, P., Ricci, L., Berner, A., Dusek, U., Galambos, Z., Mesfin, N. S., Yuskiewics, B., Wiedensohler, A., Stratmann, F. and Orsini, D. 1998a. Observed and modeled hygroscopic behavior of atmospheric particles. *Contr. Atmos. Phys.* **71**, 47–65.

Berg, O. H., Swietlicki, E. and Krejci, R. 1998b. Hygroscopic growth of aerosol particles in the marine boundary layer over the Pacific and Southern Oceans during the first Aerosol Characterization Experiment (ACE 1). *J. Geophys. Res.* **103**, D13, 16535–16545.

Berner, A. and Lürzer, C. 1980. Mass size distributions of traffic aerosols at Vienna. *J. Phys. Chem.* **84**, 2079–2083.

Birmili, W., Stratmann, F. and Wiedensohler, A. 1999. Design of a DMA-based size spectrometer for a large particle size range and stable operation. *J. Aerosol Sci.* **30**, 549–553.

Boers, R., Jenson, J. B. and Krummel, P. B. 1998. Microphysical and short-wave radiative structure of stratocumulus clouds over the Southern Ocean: Summer results and seasonal differences. *Q. J. R. Meteorol. Soc.* **124**, 151–168.

Brenguier, J. L., Chuang, P. Y., Fouquart, Y., Johnson, D. W., Parol, F., Pawlowska, H., Pelon, J., Schueller, L., Schroeder, F. and Snider, J. 2000. An overview of the ACE-2 CLOUDYCOLUMN closure experiment. *Tellus* **52B**, 815–827.

Cantrell, W., Shaw, G. and Benner, R. 1999. Cloud properties inferred from bimodal aerosol number distributions. *J. Geophys. Res.* **104**, D22, 27615–27624.

Charlson, R. J., Schwartz, S. E., Hales, J. M., Cess, R. D., Coakley, J. A., Hansen, J. E. and Hofmann, D. J. 1992.

Climate forcing by anthropogenic aerosols. *Science* **255**, 423–430.

Chuang, P. Y., Charlson, R. J. and Seinfeld, J. H. 1997. Kinetic limitations on droplet formation in clouds. *Nature*, **390**, 594–596.

Chuang, P. Y., Collins, D. R., Pawlowski, H., Snider, J. R., Jonsson, H. H., Brenguier, J. L., Flagan, R. C. and Seinfeld, J. H. 2000. CCN measurements during ACE-2 and their relationship to cloud microphysical properties. *Tellus* **52B**, 843–867.

Covert, D. S. and Heintzenberg, J. 1993. Size distributions and chemical properties of aerosol at Ny Alesund, Svalbard. *Atmos. Environ.* **27**, 2989–2997.

Cruz, C. N. and Pandis, S. N. 1998. The effect of organic coatings on the cloud condensation nuclei activation of inorganic atmospheric aerosol. *J. Geophys. Res.* **103**, D11, 13111–13123.

Faccini, M. C., Decesari, S., Mirea, M., Fuzzi, S. and Loglio, S. 2000. Surface tension of atmospheric wet aerosol and cloud/fog droplets in relation to their organic carbon content and chemical composition. *Atmos. Environ.* **34**, 4853–4857.

Ferek, R. J., Hegg, D. A., Hobbs, P. V., Durkee, P. and Nielsen, K. 1998. Measurements of ship induced tracks in clouds off the Washington coast. *J. Geophys. Res.* **103**, D18, 23199–23206.

Hudson, J. G. 1989. An instantaneous CCN spectrometer. *J. Atmos. Oceanic Technol.* **6**, 1055–1065.

Hudson, J. G., Xie, Y. and Yum, S. S. 1998. Vertical distribution of cloud condensation nuclei spectra over the summertime Southern Ocean. *J. Geophys. Res.* **103**, D13, 16609–16624.

Ji, Q. and Shaw, G. E. 1998. On supersaturation spectrum and size distributions of cloud condensation nuclei. *Geophys. Res. Lett.* **25**, 1903–1906.

Ji, Q., Shaw, G. E. and Cantrell, W. 1998. A new instrument for measuring cloud condensation nuclei: Cloud condensation nucleus remover. *J. Geophys. Res.* **103**, D21, 28013–28019.

Kulmala, M., Laaksonen, A., Charlson, R. J. and Korhonen, P. 1997. Clouds without supersaturation. *Nature* **388**, 336–337.

Laaksonen, A., Korhonen, P., Kulmala, M. and Charlson, R. J. 1998. Modification of the Koehler Equation to include soluble trace gases and slightly soluble substances. *J. Atmos. Sci.* **55**, 853–862.

Martinsson, B. G., Frank, G., Cederfelt, S. I., Berg, O. H., Mentes, B., Papaspiropoulos, G., Swietlicki, E., Zhou, J. C., Flynn, M., Bower, K. N., Choularton, T. W., Mäkelä, J., Virkkula, A. and VanDingenen, R. 2000. Validation of very high cloud droplet number concetrations in air masses transported thousands of kilometers over the ocean. *Tellus* **52B**, 801–814.

Martinsson, B. G., Karlsson, M. N. A. and Frank, G. 2001. Methodology to estimate the transfer function of individual differential mobility analyzers. *Aerosol Sci. Technol.* **35**, 815–823.

Nenes, A., Ghan, S., Abdul-Razzak, H., Chuang, P. Y. and Seinfeld, J. H. 2001. Kinetic limitations on cloud droplet formation and impact on cloud albedo. *Tellus* **53B**, 133–149.

Neusüß, C., Weise, D., Birmili, W., Wex, H., Wiedensohler, A. and Covert, D. S. 2000. Size-segregated chemical mass closure and number-derived mass closure of the marine aerosol in Sagres, Portugal. *Tellus* **52B**, 169–184.

Novakov, T. and Corrigan, C. E. 1996. Cloud condensation nucleus activity of the organic component of biomass burning smoke. *Geophys. Res. Lett.* **23**, 2141–2144.

Novakov, T. and Penner, J. E. 1993. Large contribution of organic aerosols to cloud-condensation nuclei concentrations. *Nature* **365**, 823–826.

Potukuchi, S. and Wexler, A. S. 1995. Identifying solid-aqueous phase transitions in atmospheric aerosols - I. Neutral-acidity solutions. *Atmos. Environ.* **29**, 1663–1676.

Pruppbacher, H. R. and Klett, J. D. 1997. *Microphysics of clouds and precipitation*. Kluwer Academic, Dordrecht.

Putaud, J.-P., van Dingenen, R., Mangoni, M., Virkkula, A., Raes, F., Maring, H., Prospero, J. M., Swietlicki, E., Berg, O. H., Hillamo, R. and Mäkelä, T. 2000. Chemical closure and assessment of the origin of the submicron aerosol in the marine boundary layer and the free troposphere during ACE-2. *Tellus* **52B**, 141–168.

Quinn, P. K., Anderson, T. L., Bates, T. S., Dlugi, R., Heintzenberg, J., von Hoyningen-Huene, W., Kulmala, M., Russel, P. B. and Swietlicki, E. 1996. Closure in tropospheric aerosol-climate research: A review and future needs for addressing aerosol direct shortwave radiative forcing. *Contr. Atmos. Phys.* **69**, 547–577.

Rader, D. J., and McMurry, P. H. 1986. Application of the Tandem Differential Mobility Analyzer to studies of droplet grwoth or evaporation. *J. Aerosol Sci.* **17**, 771–787.

Raes, F., Bates, T., McGovern, F. and Van Liedekerke, M. 2000. The 2nd Aerosol Characterization Experiment (ACE-2): General overview and main results. *Tellus* **52B**, 111–125.

Rogge, W. F., Mazurek, M. A., Hildemann, L. M., Cass, G. R. and Simoneit, B. R. T. 1993. Quantification of urban organic aerosols at a molecular level: Identification, abundance and seasonal variation. *Atmos. Environ.* **A27**, 1309–1330.

Saxena, P. and Hildemann, L. M. 1996. Water-soluble organics in atmospheric particles: A critical review of the literature and application of thermodynamics to identify candidate compounds. *J. Atmos. Chem.* **24**, 57–109.

Seinfeld, J. H. and Pandis, S. N. 1998. *Atmospheric chemistry and physics*. John Wiley & Sons, New York.

Shulman, M. L., Jacobson, M. C., Charlson, R. J., Syncovec, R. E. and Young, T. E. 1996. Dissolution behavior and surface tension effects of organic compounds in nucleating cloud droplets. *Geophys. Res. Lett.* **23**, 277–280.

Snider, J. R. and Brenguier, J.-L. 2000. Cloud condensation nuclei and cloud droplet measurements during ACE-2. *Tellus* **52B**, 828–842.

Stolzenburg, M. R. and McMurry, P. H. 1988. *TDMAFIT user's manual*. PTL Publications N0. 653, Particle Technology Laboratory Department of Mechanical Eng., University of Minnesota, Minneapolis, USA.

Swietlicki, E., Zhou, J., Berg, O. H., Martinsson, B. G., Frank, G., Cederfelt, S. I., Dusek, U., Berner, A., Birmili, W., Wiedensohler, A., Yuskiewicz, B. and Bower, K. N. 1999. A closure study of sub-micrometer aerosol particle hygroscopic behavior. *Atmos. Res.* **50**, 205–240.

Swietlicki, E., Zhou, J., Covert, D. S., Hämeri, K., Busch, B., Väkeva, M., Dusek, U., Berg, O. H., Wiedensohler, A., Aalto, P., Mäkelä, J., Martinsson, B. G., Papaspiropoulos, G., Mentes, B., Frank, G., and Stratmann, F. 2000. Hygroscopic properties of aerosol particles in the northeastern Atlantic during ACE2. *Tellus* **52B**, 201–227.

Tang, I. N. 1997. Thermodynamic and optical properties of mixed-salt aerosols of atmospheric importance. *J. Geophys. Res.* **102**, D2, 1883–1893.

Tang, I. N. and Munkelwitz, H. R. 1994. Water activities, densities and refractive indices of aqueous sulfate and sodium nitrate droplets of atmospheric importance. *J. Geophys. Res.* **99**, D9, 18801–18808.

Twomey, S. 1959. The nuclei of natural cloud formation, Part II: the supersaturation in natural clouds and variation of cloud droplet concentration. *Geofis. Pura Appl.* **43**, 243–249.

Twomey, S. 1991. Aerosols, clouds and radiation. *Atmos. Environ.* **25**, 2435–2442.

Twomey, S., Gall, R. and Leuthold, M. 1987. Pollution and cloud reflectance. *Boundary Layer Meteorol.* **41**, 335–348.

Verver, G., Raes, F., Vogelzang, D. and Johnson, D. 2000. The 2nd Aerosol Characterization Experiment (ACE-2): Meteoroogical and chemical context. *Tellus* **52B**, 126–140.

Vong, R. J. and Covert, D. S. 1998. Simultaneous observations of aerosol and cloud droplet size spectra in marine stratocumulus. *J. Atmos. Sci.* **55**, 2180–2192.

Wood, R., Johnson, D., Osborne, S., Andreae, M. O., Bandy, B., Bates, T. S., O'Dowd, C., Glantz, P., Noone, K. J. and Quinn, P. K. 2000. Boundary layer and aerosol evolution during the 3rd Lagrangian experiment of ACE-2. *Tellus* **52B**, 401–422.

Yamasoe, M. A., Artaxo, P., Miguel, A. H. and Allen, G. 2000. Chemical composition of aerosol particles from direct emissions of vegetation fires in the Amazon Basin: water-soluble species and trace elements. *Atmos. Environ.* **34**, 1641–1653.